Original Article

Arsenic enhances cervical cancer cell radiosensitivity by suppressing the DNA damage repair pathway

Xingxing Gao[1#], Genyun Liu[1#], Zimu Zhao[2#], Yi Tang[1], Hui Hui[1], Chaoqun Wang[2], Danhua Li[2], Yu Ma[2], Zhuo Sun[2], Yun Zhou[1]

[1]The Affiliated Xuzhou Clinical College of Xuzhou Medical University, Xuzhou, China; [2]Department of Pathology, School of Basic Medical Sciences, Xuzhou Key Laboratory of Clinical and Experimental Pathology, Xuzhou Medical University, Xuzhou, China

Contributions: (I) Conception and design: X Gao, Z Sun, Y Zhang; (II) Administrative support: C Wang, D Li, Y Ma; (III) Provision of study materials or patients: X Gao, G Liu, Z Zhao; (IV) Collection and assembly of data: X Gao, H Huang, Y Tang; (V) Data analysis and interpretation: G Liu, Z Zhao, C Wang, Y Tang; (VI) Manuscript writing: All authors; (VII) Final approval of manuscript: All authors.

[#]These authors contributed equally to this work.

Correspondence to: Professor Zhuo Sun, PhD. Department of Pathology, School of Basic Medical Sciences, Xuzhou Key Laboratory of Clinical and Experimental Pathology, Xuzhou Medical University, 209 Tongshan Road, Xuzhou 221004, China. Email: sunzhuo@xzhmu.edu.cn; Professor Yun Zhou, PhD. The Affiliated Xuzhou Clinical College of Xuzhou Medical University, 199 Jiefangnan Road, Xuzhou 220005, China. Email: zhouyun-0528@163.com.

Background: Concurrent chemoradiotherapy (CCRT) is a primary treatment for cervical cancer (CC) and combines chemotherapy and radiation therapy to target cancer cells effectively. However, despite its benefits, it also involves a high risk of recurrence and metastasis, partly due to the resistance of some cancer cells to the treatment. Additionally, CCRT can cause various treatment-related adverse reactions, such as gastrointestinal issues, bone marrow suppression, and skin reactions, which can negatively impact patients' quality of life. Therefore, there is a compelling need to develop more effective treatment strategies that can improve the outcomes of CCRT while minimizing its side effects. This study aimed to investigate the radiosensitizing effects of arsenic trioxide (ATO) on CC and explore its underlying molecular mechanisms.

Methods: We conducted both *in vitro* and *in vivo* experiments to evaluate the radio-sensitizing properties of ATO. The *in vitro* effects of ATO were assessed using clonogenic assay, while *in vivo* effects were evaluated using a xenograft model. Then cell viability, cell cycle, and apoptosis were assessed by Cell Counting Kit-8 (CCK-8) assay and flow cytometry. RNA sequencing was performed to identify the differentially expressed genes. Finally, mRNA and protein expressions of key hub genes were analyzed by quantitative real-time polymerase chain reaction (qRT-PCR) and western blot. Western blot, immunofluorescence, and RNA sequencing analyzed molecular mechanisms.

Results: ATO significantly enhanced the radiosensitivity of CC cells, as evidenced by reduced colony formation *in vitro* and inhibited tumor growth *in vivo*. This enhancement was achieved by impairing the DNA damage repair pathway, specifically through the downregulation of key proteins such as breast cancer 1 (*BRCA1*) and bloom syndrome protein (*BLM*). Notably, overexpression of BRCA1 or BLM substantially mitigated ATO's radiosensitizing effects.

Conclusions: This study demonstrates that ATO exhibits radiosensitizing effects on CC by inhibiting DNA damage repair. These findings provide theoretical and experimental support for using ATO as a radiosensitizer in CC therapy, potentially leading to improved treatment outcomes, reduced recurrence rates, and enhanced patient survival. Future research should focus on optimizing ATO's dosage and timing as well as evaluating its long-term safety and efficacy in clinical settings.

Keywords: Cervical cancer (CC); radiotherapy; arsenic trioxide (ATO); radiosensitize; DNA damage repair

Submitted Feb 28, 2025. Accepted for publication Mar 19, 2025. Published online Mar 27, 2025.
doi: 10.21037/tcr-2025-450
View this article at: https://dx.doi.org/10.21037/tcr-2025-450

Introduction

Cervical cancer (CC) is the most prevalent malignancy of the female reproductive system, posing a significant threat to women's health and life (1). The initial manifestations of cervical carcinoma are often subtle, leading to the majority of cases being identified at advanced stage. Consequently, the therapeutic window for surgical intervention is frequently missed, thereby adversely affecting the patient's prognosis and treatment options. Radiotherapy is one of the most common therapeutic interventions for CC (2). However, radiotherapy alone is often marred by issues such as a low local control rate and a high distant metastasis rate, leading to an unsatisfactory 5-year survival rates for patients (3). A large number of studies have shown that comprehensive radiotherapy is significantly better than is radiotherapy alone, especially concurrent chemoradiotherapy (CCRT) based on platinum, which can significantly improve the prognosis of patients and has become the main treatment method for advanced CC. However, in clinical work, CCRT is associated with numerous challenges, including significant bone marrow suppression, gastrointestinal reactions, and renal toxicity (4,5). Furthermore, a subset of patients exhibits a diminished response to platinum-based therapies, which predominantly attributed to the elevated antioxidant capacity of CC cells [(I) NRF2/KEAP1 signaling inhibitors in gynecologic cancers. (II) Targeting the NRF2/KEAP1 pathway in cervical and endometrial cancers]. These issues can all lead to treatment failure. Hence, there is an urgent need to develop lower-toxicity and higher-efficiency chemotherapy drugs and corresponding treatment strategies.

Arsenic trioxide (ATO), the main component of the traditional Chinese medicine known as "Pishuang", has historically been used to treat conditions such as psoriasis, syphilis, rheumatism, and malaria (6). However, due to its toxicity, ATO was not extensively applied in clinical settings until its high efficacy in treating acute promyelocytic leukemia (APL) was established (7,8). Subsequently, researchers have been continuously exploring its application in the experimental treatment of other hematologic malignancies, lymphomas, and solid tumors, which has yielded promising therapeutic outcomes (9-11). The antitumor effect of ATO has therefore received increased attention in recent years.

The anticancer efficacy of ATO can be predominantly attributed to its multifaceted biological activities, which include the induction of apoptosis, suppression of cell proliferation, and the promotion of incomplete cytodifferentiation (12,13). However, an increasing number of studies have also indicated that arsenic may disrupt a wide array of other biological processes, including histone deacetylase activity, cell cycle progression, DNA repair, ubiquitination, tubulin polymerization, nitric oxide synthesis, and the expression or activation of oncogenes (14,15). In our previous work, we also found that ATO could activate autophagy by upregulating the expression of FoxO3a, thereby inhibiting tumor angiogenesis (16,17). Moreover, recent research has suggested that ATO could also act as a radiosensitizer in the radiotherapy of some tumors. Earlier investigations in this field showed that the use of ATO to treat skin metastatic lesions in patients with breast cancer before radiotherapy could enhance the therapeutic effect of radiotherapy (18). Kumar *et al.* found that ATO could significantly enhance the therapeutic effect of radiotherapy on oral squamous cell carcinoma while reducing radiation-induced bone loss (19). Another study on pancreatic cancer found that ATO and dimercaprol could significantly enhance the inhibitory effect of radiotherapy on xenotransplanted pancreatic tumors (20). In addition, several other arsenic compounds, including arsenates and arsenic sulfide, also exert a radiosensitizing effect on glioblastoma and rhabdomyosarcoma (21,22). These studies collectively suggested that ATO could be used in combination with chemotherapy drugs and radiotherapy to

Highlight box

Key findings

- Our study confirmed the radiosensitizing activity of arsenic trioxide (ATO) in cervical cancer (CC) cells.

What is known and what is new?

- Concurrent chemoradiotherapy is a primary treatment for CC, but it has high risks of recurrence and metastasis and various adverse reactions. Studies have shown that ATO can potentiate the effects of radiotherapy in treating tumors, suggesting its potential application as a radiosensitizer.
- This study demonstrated that ATO enhances CC cell radiosensitivity by inhibiting DNA repair genes *BRCA1* and *BLM*, representing a novel finding in CC treatment.

What is the implication, and what should change now?

- Our findings indicate that ATO's radiosensitizing effect at nontoxic doses could improve radiotherapy outcomes in CC, and the implications of the study include a potential shift in the treatment paradigm for CC, with a focus on more targeted, less toxic, and potentially more effective therapies. These innovations should be guided by further research and clinical validation.

further enhance its therapeutic effect on tumors.

However, the application of ATO in the radiotherapy of CC remains an underexplored area, with the dosage and therapeutic regimen requiring further refinement. The molecular underpinnings of ATO's radiosensitizing effects in the context of tumor radiotherapy have yet to be comprehensively elucidated. Therefore, in this study, we examined the radiosensitizing effects of ATO on human CC cells and clarified the relevant molecular mechanisms. The findings of this study may offer a theoretical framework and empirical insights, contributing novel perspectives and methodologies for the clinical utilization of ATO in radiotherapeutic approaches. We present this article in accordance with the ARRIVE and MDAR reporting checklists (available at https://tcr.amegroups.com/article/view/10.21037/tcr-2025-450/rc).

Methods

Reagents and antibodies

Fetal bovine serum (FBS) was purchased from Tianhang Biotechnology (13011-8611, Huzhou, China). Dulbecco's Modified Eagle Medium (DMEM; KGL1206) and trypsin (KGL2101) were purchased from Keygen Biotech (Nanjing, China). ATO was purchased from Harbin Medical University Pharmaceutical Co., Ltd. (H19990191, Harbin, China). Cell Counting Kit-8 (CCK-8; KGA-9305), Annexin V/propidium iodide (PI) Detection Kit (KGA-1101) and Cell Cycle Detection Kit (KGA-9101) were purchased from KeyGen Biotech (Nanjing, China). Primary antibodies against breast cancer 1 (*BRCA1*) (bs-20490R) and bloom syndrome protein (*BLM*) (bs-12872R) were purchased from Bioss Biotech (Boston, MA, USA). γ-H2AX (ab81299), glyceraldehyde 3-phosphate dehydrogenase (GAPDH; 10494-1-AP), and tubulin (10094-1-AP) were purchased from Proteintech Group (Chicago, IL, USA). Horseradish peroxidase (HRP)-conjugated secondary antibodies (BF03001, BF03008) were purchased from Santa Cruz Biotechnology Inc. (Santa Cruz, CA, USA). Fluorescence-conjugated secondary antibody (A32731) was purchased from Invitrogen (Thermo Fisher Scientific, USA).

Cell culture

SiHa (TCHu113) and HeLa (TCHu187) cells were obtained from the Shanghai Cell Bank of the Chinese Academy of Sciences (Shanghai, China). Cells were cultured in DMEM supplemented with 10% FBS and maintained in an incubator containing 5% CO_2 at 37 ℃.

Cell viability assay

Cells (2×10^4 cells/well) were seeded in a 96-well plate. After attachment, the cells were treated with different concentrations of ATO or vehicle control for 24 hours. Subsequently, 10 µL of CCK-8 reagent was added to each well and incubated for 2 hours at 37 ℃. The optical density (OD) at 450 nm was measured using a microplate reader (Thermo Fisher Scientific). The cell survival rate was calculated using the following formula: cell survival rate = (experimental group OD – blank group OD)/(control group OD – blank group OD) × 100%.

Clonogenic assay

Cells were prepared into a single-cell suspension and then seeded into a six-well plate. Five irradiation (IR) doses were set, including 0, 2, 4, 6, and 8 Gy, with 200, 300, 400, 600, and 800 cells seeded per well, respectively. ATO was added after the cells adhered to the plate, and IR was performed 24 hours later. After IR, the cells were cultured for 14 days, fixed with 4% paraformaldehyde, permeated with 20% methanol, and stained with crystal violet. Colonies with more than 50 cells were counted under a microscope, and statistical analysis was performed. The survival fraction (SF) was calculated using the following formula: SF = treated group clonogenic rate/control group clonogenic rate. The radiation sensitizer enhancement ratio (SER) was calculated using the multitarget single-hit model as follows: $SF = 1 - (1 - e^{-D/D0})^N$, where D is the radiation dose, and D0 is the lethal dose; meanwhile, the quasithreshold dose (Dq) was calculated as follows: $Dq = D_0 \log N$, where N is the extrapolation number.

Cell cycle analysis

After specific treatment, 1×10^6 cells were collected, washed twice with phosphate-buffered saline (PBS) and fixed with 70% cold ethanol overnight at 4 ℃. After removal of the fixation buffer, 100 µL of RNase A and 400 µL of PI were added, and the cells were incubated at 4 ℃ in the dark for another 20 minutes. Cell cycle was detected using a flow cytometer flow cytometer (BD FACSCalibur) and analyzed by FlowJo Software (BD Biosciences, Franklin Lakes, NJ, USA).

Apoptosis assay

After specific treatment, 1×10^6 cells were collected, washed twice with PBS, and resuspended in 500 µL of binding buffer. Subsequently, 5 µL of Annexin V-Fluorescein Isothiocyanate (FITC) and 5 µL of PI were added and incubated in the dark for 10 minutes. Apoptosis was detected using a flow cytometer flow cytometer (BD FACSCalibur) and analyzed by FlowJo Software (BD Biosciences). Cells stained positive for Annexin V were considered to be apoptotic cells.

Western blot analysis

Cells were lysed in radioimmunoprecipitation assay (RIPA) buffer and quantified using a bicinchoninic acid (BCA) protein quantitation kit (KGB-2101, Ketgen Biotech, Nanjing, China). Total proteins (30 µg per lane) were separated via sodium dodecyl sulfate-polyacrylamide gel electrophoresis and transferred to polyvinylidene fluoride (PVDF) membranes. After blocking with 5% nonfat milk in Tris-buffered saline with Tween20 (TBS-T), the membranes were incubated with primary antibodies overnight at 4 ℃ and then with a secondary antibody for 2 hours at room temperature. Finally, the immune complexes were detected using an enhanced chemiluminescence system.

Immunofluorescence staining

After specific treatment, cells were fixed with 4% paraformaldehyde for 10 minutes and then permeabilized with 0.5% Triton X-100 at room temperature for 20 minutes. After blocking with 5% goat serum for 30 minutes, the primary antibody was diluted 1:200 in PBS and incubated at 4 ℃ overnight. The cells were then washed again and incubated with fluorescence-conjugated secondary antibodies for 2 hours at room temperature. Before observation, the nuclei were counterstained with 4'-6-diamidino-2-phenylindole (DAPI), and the results were then analyzed by fluorescence microscopy (Leica, Wetzlar, Germany).

RNA sequencing and bioinformatics analysis

For the control group, IR group, ATO group, and ATO + IR group, RNA sequencing was performed, and gene data were obtained from the GeneDio Bioinformatics Platform (https://www.genedenovo.com/). Differential genes and functional enrichment were compared between the control and IR groups and between the IR and ATO + IR groups. All bioinformatics analysis were performed using the Omicsmart online platform (http://www.omicsmart.com). Protein-protein interaction (PPI) network analysis of differentially expressed genes (DEGs) in the DNA repair pathway was constructed using the Search Tool for the Retrieval of Interacting Genes/Proteins (STRING) online database (http://string-db.org/).

Quantitative polymerase chain reaction (qPCR)

Total RNA was extracted using TRI Reagent (AM9738, Invitrogen) according to the manufacturer's instructions. A total of 1 µg of RNA was used for complement DNA (cDNA) synthesis and cDNA was generated via HiScript II RT SuperMix (R232-01, Vazyme Biotech, Nanjing, China). An equal amount of cDNA was applied for quantitative real-time PCR (qRT-PCR) analysis with AceQ qPCR SYBR Green Master Mix (Q121-02, Vazyme) in a StepOnePlus Real-Time PCR System (Applied Biosystems, Thermo Fisher Scientific) under the following conditions: 5 minutes at 95 ℃, followed by 40 cycles of 15 seconds at 95 ℃ and 30 seconds at 60 ℃. GAPDH was used as a control. The primer sequences are listed in *Table 1*.

Establishment of the xenograft model

Cells were collected and prepared into a cell suspension at a concentration of 1×10^7 cells/mL. Cell suspension (100 µL) was injected into the right axillary region of healthy female BALB/c nude mice (6 weeks old; NOD/ShiLtJGpt-Prkdcem26Cd52Il2rgem26Cd22/Gpt; Jicui Pharmachem, Shanghai, China). When the subcutaneous tumors in the nude mice grew to approximately 0.01 cm^3, 20 mice with uniform tumor sizes were selected, randomly divided into 4 groups (control, IR, ATO, and ATO + IR) using a computer-generated sequence, and then subjected to different drug and radiotherapy treatments. To minimize potential confounding factors: mice from different groups were housed in separate cages with randomized cage positions within the animal facility to avoid cage effects. All experimental procedures, including drug administration, irradiation, and tumor measurements, were performed by researchers blinded to group assignments. Group assignments were decoded only after data analysis. The laboratory environment was maintained at a constant

Table 1 Primer sequences for qRT-PCR

Gene	Forward primer (5'→3')	Reverse primer (5'→3')
BRCA1	CCACAGTCGGGAAACAAGCATAGA	CTTCTGCATTTCCTGGATTTGAAACC
BLM	GAGTCTGCGTGCGAGGATTA	AGTGTTCTGGCTGAGTGACG
MCM7	ACTGAAGGACTACGCGCT	CTTTCCCGACAGAGACCACTC
FANCL	AATCCCCCGATTCCACCAAC	TGCGTTGTAAGATTTATTTTGGCT
WRN	GCATGCACTTATCCCAAGCG	GTTGAAGTCCGCTGTCAGGA
GAPDH	CCAACGTGTCTGTTGTGGATCTGA	GAGCTTGACAAAGTGGTCGTTGAG

BLM, bloom syndrome protein; BRCA1, breast cancer 1; FANCL, Fanconi anemia, complementation group l; GAPDH, glyceraldehyde 3-phosphate dehydrogenase; MCM7, minichromosome maintenance complex component 7; qRT-PCR, quantitative real-time polymerase chain reaction; WRN, Werner syndrome RecQ-like helicase.

temperature (23±1 ℃) and humidity (50%±5%) with a standardized 12-hour light-dark cycle throughout the study. These measures aimed to control for environmental variability, observer bias, and spatial confounding. ATO SiHa (4 mg/kg) was administered via the tail vein on days 2, 4, 6, 10, and 13, and IR (4 Gy) was performed 24 hours after ATO injection. Starting from the day of the first drug administration, the length (a) and width (b) of the tumor were measured every 3 days. On the 31st day after cell inoculation, the nude mice were euthanized using carbon dioxide, the tumors were excised, and the tumor volume (V) was calculated using the following formula: $V = a \times b^2/2$. The tumor growth curve was subsequently plotted. Samples of the main organs of the mice were collected and fixed for subsequent experiments.

Experiments were performed under a project license (No. 202305T019) granted by the approval of the Animal Care and Use Committee of Xuzhou Medical University, in compliance with national guidelines for the care and use of animals. A protocol was prepared before the study without registration.

Statistical analysis

All statistical analyses were performed using GraphPad Prism (Dotmatics, Boston, MA, USA). Numerical data from three independent experiments are represented as the mean ± standard deviation (SD). Comparisons between two groups were made using two-tailed Student *t*-tests, and multiple comparisons were performed using analysis of variance (ANOVA). $P<0.05$ was considered to indicate statistical significance.

Results

ATO exerted a dose-dependent cytotoxic effect on SiHa and HeLa cells in vitro

Considering the side effects of ATO, we first evaluated the cytotoxic effect of ATO on SiHa and HeLa, two human CC cell lines. Cells were exposed to varying concentrations of ATO, and their viability was assessed 24 hours posttreatment via CCK-8 assays. There was a significant reduction in cell viability for both SiHa and HeLa cell lines at ATO concentrations equal to or exceeding 1 μM (*Figure 1*) in a dose-dependent manner. To minimize the cytotoxic effect of ATO, 1 μM ATO was selected for further study.

ATO radiosensitized SiHa and HeLa in vitro and in vivo

To determine whether ATO exposure sensitizes CC cells to IR, clonogenic survival assays were performed. Cells were pretreated with ATO for 24 hours prior to their exposure to different doses of IR. After the cells were cultured for 15 days, a multitarget single-hit model was used to assess the radiosensitizing effect of ATO on SiHa and HeLa cells. Our findings demonstrated that ATO treatment significantly reduced the levels of colony formation following IR. According to the parameters of radiosensitization shown in *Tables 2*,*3*, ATO treatment exhibited higher sensitivity enhancement ratio (SER DEG) in both SiHa and HeLa cells (SER SiHa =1.37; SER Hela =1.30) (*Figure 2A*,*2B* and *Tables 2*,*3*).

To further substantiate the above findings, we investigated the radiosensitizing effect of ATO on CC *in vivo*. To this end, a xenotransplantation model of human

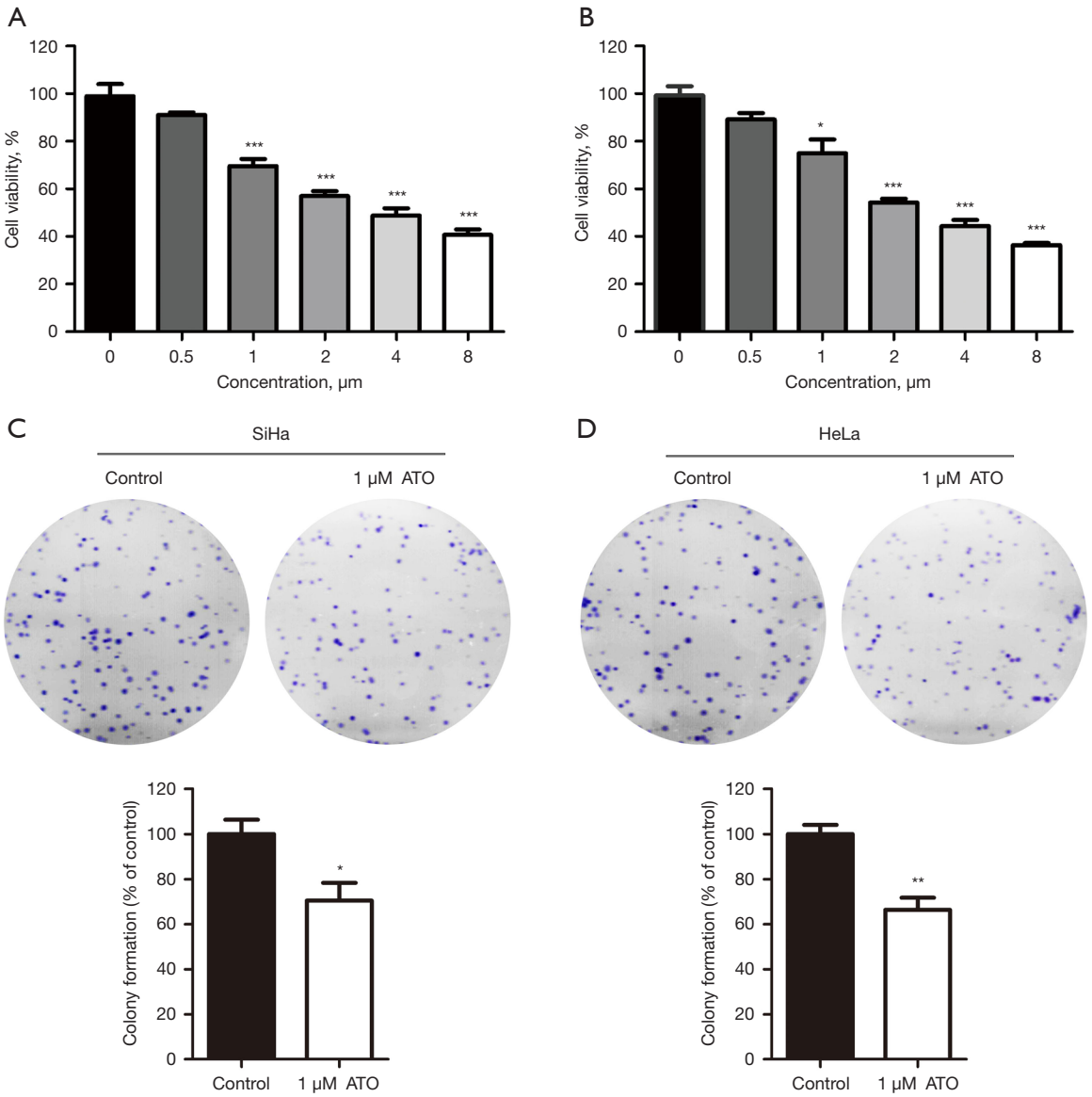

Figure 1 ATO exerted a dose-dependent cytotoxic effect on SiHa and HeLa cells *in vitro*. (A) SiHa and (B) HeLa cells were treated with different concentrations of ATO for 24 hours. The cell viability was then measured with the CCK-8 assay. Representative colony formation assays of SiHa (C) and HeLa (D) cells. Lower panels are quantitative analysis of colony formation assay. Colonies formed were stained with crystal violet and determined under a microscope (×1 magnification). All data are representative of at least three independent experiments (n≥3). *, P<0.05; **, P<0.01; ***, P<0.001 *vs.* control group. ATO, arsenic trioxide; CCK-8, Cell Counting Kit-8.

Table 2 Principal parameters of SiHa cell survival curve after irradiation

Group	D0 (Gy)	Dq (Gy)	SER
Control	1.54	3.47	1.37
ATO	1.27	2.54	–

D0: mean lethal dose. Dq: quasithreshold dose. ATO, arsenic trioxide; SER, sensitizer enhancement ratio.

Table 3 Principal parameters of HeLa cell survival curve after irradiation

Group	D0 (Gy)	Dq (Gy)	SER
Control	1.63	3.25	1.30
ATO	0.95	2.50	–

D0: mean lethal dose. Dq: quasithreshold dose. ATO, arsenic trioxide; SER, sensitizer enhancement ratio.

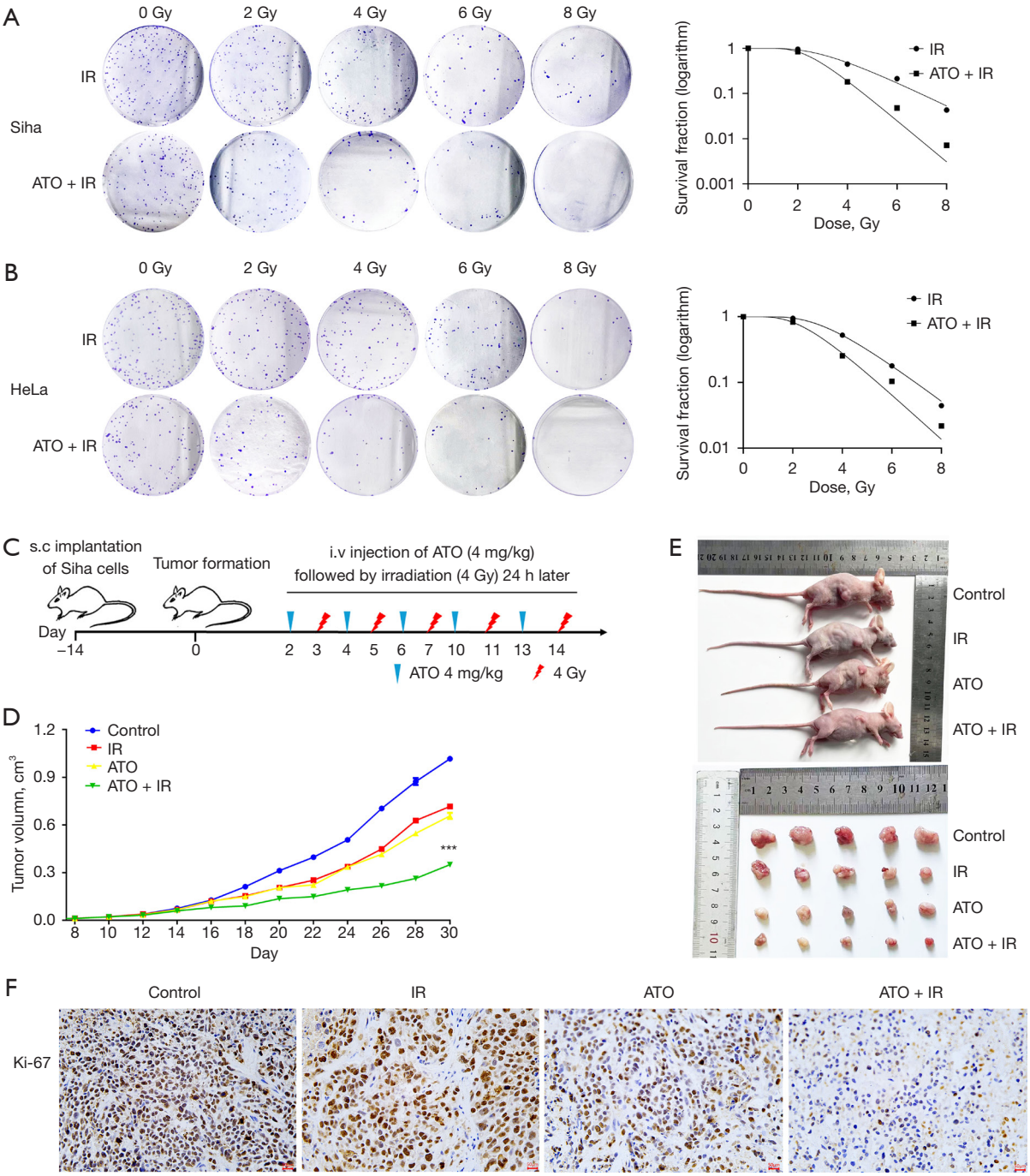

Figure 2 ATO radiosensitized SiHa and HeLa *in vitro* and *in vivo*. Representative (left) image and (right) quantitative analysis of the colony formation assay in (A) SiHa and (B) HeLa cells. Data are presented as mean ± SD from three independent experiments (n=3). Radiosensitization of SiHa and HeLa cells was analyzed via clonogenic assay after treatment with ATO for 24 hours followed by irradiation with doses of 0, 2, 4, 6, or 8 Gy. Colonies formed were then stained with crystal violet and determined under a microscope (×1 magnification). (C) Schematic showing the schedules of ATO treatment and radiotherapy. (D) Average tumor volumes of the mice in different treatment groups during the experimental period. ***, P<0.001. (E) Upper panel: xenograft tumors for 26med in nude mice in different treatment groups. Lower panel: images of the tumor tissues obtained from each group (n=5). (F) IHC staining of Ki-67 in tumor tissues from the mice in the different treatment groups. ATO, arsenic trioxide; IHC, immunohistochemistry; IR, irradiation; i.v., intravenous; s.c., subcutaneous; SD, standard deviation.

CC was established in Balb/c nude mice using SiHa cells. After tumors reached approximately 0.01 mm^3 in volume, experiment mice groups received IR and/or ATO treatment (*Figure 2C*). As illustrated in *Figure 2D,2E*, the combined treatment of ATO and IR markedly inhibited the growth of SiHa tumors in comparison to the control group, as well as the groups receiving ATO or IR alone. This suggests that ATO treatment enhances the sensitivity of the CC model to IR. Furthermore, we conducted an analysis of Ki-67 expression, a marker of cellular proliferation, in tumor tissues extracted from both treated and untreated mice at the endpoint of the experiment. Consistent with our expectations, the Ki-67 expression levels were significantly reduced in the group receiving the combined IR and ATO treatment compared to the group receiving monotherapy (*Figure 2F*).

Collectively, these findings demonstrate that pretreatment with ATO significantly augments the radiosensitivity of CC both *in vitro* and *in vivo*.

ATO enhanced IR-induced cell cycle arrest and cell apoptosis

We then further evaluated the effect of ATO on the cell cycle and apoptosis, both of which play pivotal roles in radiosensitivity. Analysis of the cell cycle using flow cytometry revealed that the co-treatment with ATO and a 4-Gy X-ray IR resulted in a significant increase in G2/M phase arrest in both SiHa and HeLa cells (*Figure 3A,3B*). Furthermore, the Annexin V-FITC/PI double-staining assay indicated that ATO treatment alone heightened the incidence of apoptosis in both cell types, with a markedly pronounced effect observed upon its combination with IR (*Figure 3C,3D*).

These data suggested that ATO treatment combined with IR may enhance the radiosensitivity of CC cells by activating the G2/M checkpoint and inducing increased apoptosis.

ATO inhibited DNA damage repair in irradiated CC cells

Apoptosis and cell cycle arrest in tumor cells following radiation exposure are believed to be triggered by DNA double-strand breaks (DSBs), which are the most critical form of radiation-induced damage. However, DSBs can be effectively repaired through various DNA repair mechanisms. Given that the capacity for DNA repair is closely linked to the outcomes of radiotherapy, we then conducted an assessment of DSBs in irradiated cells through the γH2AX foci formation assay (a biomarker indicative of DSBs).

As delineated in *Figure 4A,4B*, both IR and ATO significantly induced DNA damage, evidenced by an increase in γH2AX foci formation within SiHa and HeLa cells. Moreover, the combination of ATO with IR elicited a pronounced enhancement in the formation of γ-H2AX foci. These findings suggested that the combination of ATO with IR resulted in more profound DNA damage, which subsequently led to an increase in the cancer-killing effect.

ATO suppressed the DNA damage repair signaling pathway

To further clarify the mechanism underlying the ATO-mediated cellular radiosensitivity, groups of CC cells, including control, IR, ATO + IR, and ATO, were subjected to conduct RNA sequencing. A heatmap and scatter plot (*Figure 5A,5B*) were used to visualize the profiles of the DEGs (fold change >2.0 and P<0.05) among these groups, while volcano plots (*Figure 5C*) were used to demonstrate the profiles of the differentially expressed RNAs (fold change >2.0 and P<0.05) between the control and IR group and between the IR and ATO + IR group. A total of 1,590 DEGs were detected between the control and IR group (1,476 were upregulated, and 114 were downregulated), and 147 DEGs were detected between the IR and ATO + IR group (45 were upregulated, and 102 were downregulated). Gene Ontology (GO) pathway enrichment analysis revealed that the DEGs predominantly originated from genes significantly associated with cellular processes biological process (BP), binding molecular function (MF), and cellular anatomical entity cellular component (*Figure 5D*). To further verify the effect of ATO on DNA damage repair pathway, gene set enrichment analysis (GSEA) of gene sets for DNA repair were conducted and indicated that DNA repair-related genes were enriched after IR, while negative regulation of DNA repair was enriched in the ATO + IR group as compared with IR only group; this confirmed the suppression of DNA damage repair signaling via ATO treatment (*Figure 5E*). To predict the key hub genes involved in the radiosensitizing effect of ATO, an analysis of the PPI network for the DEGs within the DNA repair pathway was conducted via the STRING database. Based on the PPI network analysis, *BRCA1*, *BLM*, Fanconi anemia, complementation group I (*FANCI*), and Werner syndrome RecQ-like helicase (*WRN*) were identified as the key hub genes (*Figure 5F*).

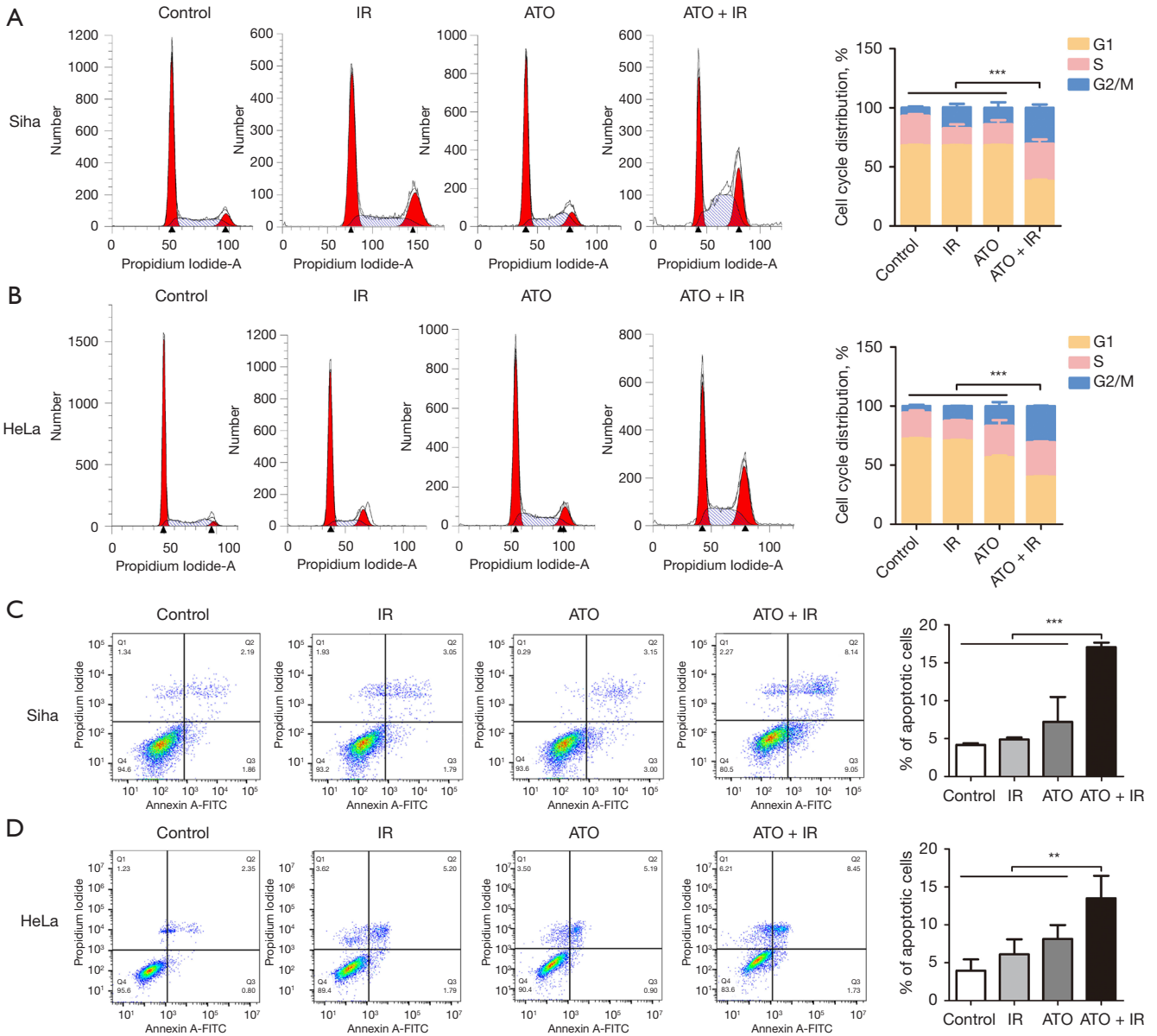

Figure 3 ATO enhanced IR-induced cell cycle arrest and cell apoptosis. The cell cycle distribution of (A) SiHa and (B) HeLa cells were analyzed by flow cytometry combined with propidium iodide following the indicated treatment. The percentage of the cell population in different phases of the cell cycle was determined and plotted in a bar graph. Annexin-V/PI double-stain for the cell apoptosis of (C) SiHa and (D) HeLa cells were measured by flow cytometry following the indicated treatment. (A,B) Bar graph for the percentage of the cell population in early and late apoptosis. All plot data are expressed as the mean ± SD (n≥3). **, P<0.01; ***, P<0.001. ATO, arsenic trioxide; FITC, fluorescein isothiocyanate; IR, irradiation; PI, propidium iodide; SD, standard deviation.

The radiosensitizing effect of ATO was facilitated by its interference with the DNA repair mechanism

We validated the expression of key hub genes in DNA damage repair signaling pathway by qRT-PCR and Western blot assays in SiHa cells. As shown in *Figure 6A*, DNA damage repair-related genes *BRCA1* and *BLM* were significantly downregulated after combined treatment of ATO with IR. Western blot assay also showed suppressed

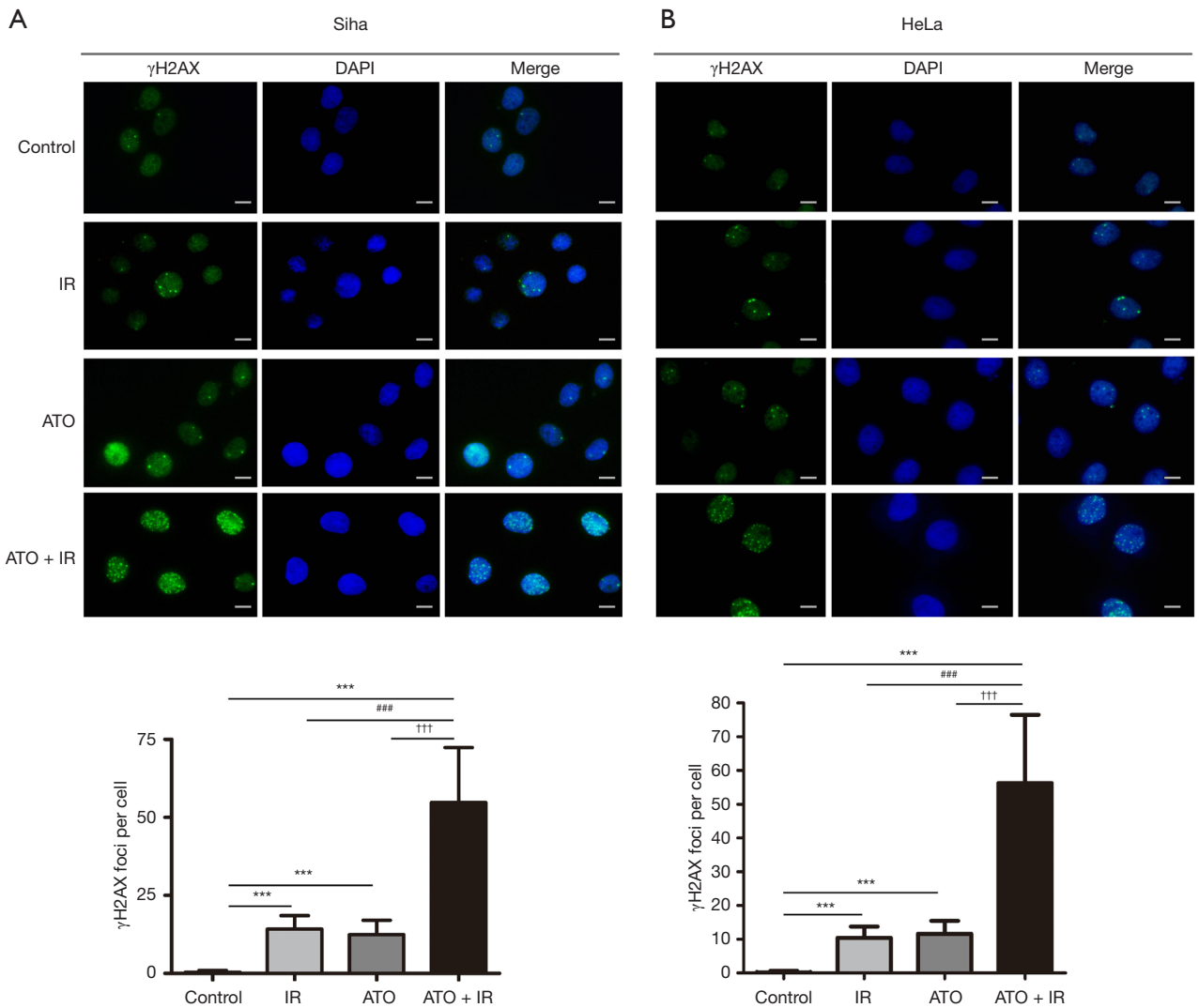

Figure 4 ATO inhibited DNA damage repair in irradiated cervical cancer cells. Representative images of γH2AX immunofluorescent staining in (A) SiHa and (B) HeLa cells following the indicated treatment (scale bar, 10 μm). The histograms show the average numbers of γH2AX foci per cell in different treatment groups. Nuclei were stained blue with DAPI (n=3). ***, P<0.001 *vs.* control group; ###, P<0.001 *vs.* IR group; †††, P<0.001 *vs.* ATO group. ATO, arsenic trioxide; DAPI, 4'-6-diamidino-2-phenylindole; IR, irradiation.

BRCA1 and BLM protein levels in SiHa cells after IR combined with ATO (*Figure 6B*). These results suggested that ATO likely enhances radiosensitizing effect by impairing the DNA damage repair pathway.

To substantiate this speculation, we employed plasmid transfection to overexpress BRCA1 or BLM in SiHa cells, followed by treatment with IR and ATO. Subsequent Western blot analysis was conducted to quantify the expression levels of BRCA1 and BLM proteins across the various cell groups. The findings revealed that overexpression notably restored the levels of BRCA1 or BLM proteins that were diminished by the combined treatment of IR and ATO (*Figure 6C*). Clonogenic survival assays further indicated that ATO significantly enhanced the radiosensitivity of SiHa cells. Conversely, the overexpression of BRCA1 or BLM substantially mitigated the radiosensitizing effect of ATO, effectively reverting the SF of SiHa cells to levels akin to those observed in the group treated with IR only, as evidenced by the SER values of 0.9 *vs.* 1.32 in the BRCA1-overexpression group and 1.04

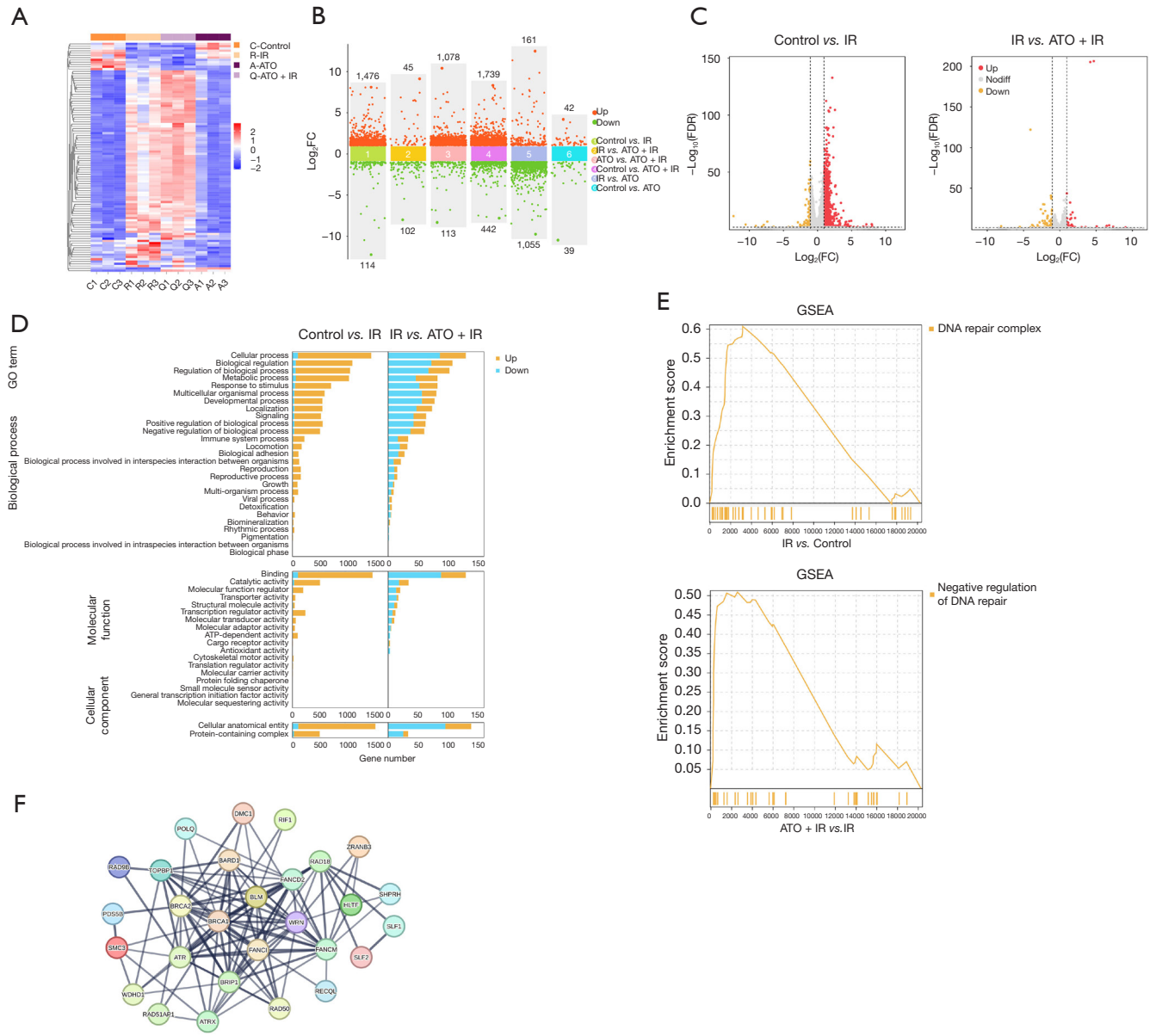

Figure 5 ATO suppressed the DNA damage repair signaling pathway. (A) Heatmap of the DEGs in different treatment groups. (B) Scatter plot of the DEGs in the indicated comparison pairs. (C) Volcano plot of the DEGs for control *vs.* IR and for IR *vs.* ATO + IR. (D) GO enrichment analysis the DEGs for control *vs.* IR and for IR *vs.* ATO + IR. (E) GSEA results. (F) PPI network of the DEGs within the DNA repair pathway constructed via STRING. IR, irradiation; ATO, arsenic trioxide; DEGs, differentially expressed genes; FC, fold change; FDR, false discovery rate; GO, Gene Ontology; GSEA, gene set enrichment analysis; IR, irradiation; PPI, protein-protein interaction; STRING, Search Tool for the Retrieval of Interacting Genes/Proteins.

vs. 1.27 in the BLM-overexpression group, respectively (*Figure 6D*; *Tables 4*,*5*). Collectively, these outcomes provided further validation that ATO's radiosensitizing effects were primarily mediated through the inhibition of the DNA damage repair pathway.

Discussion

CCRT is one of the primary methods for treating CC. However, it is associated with certain drawbacks, such as a high risk of recurrence and metastasis and treatment-

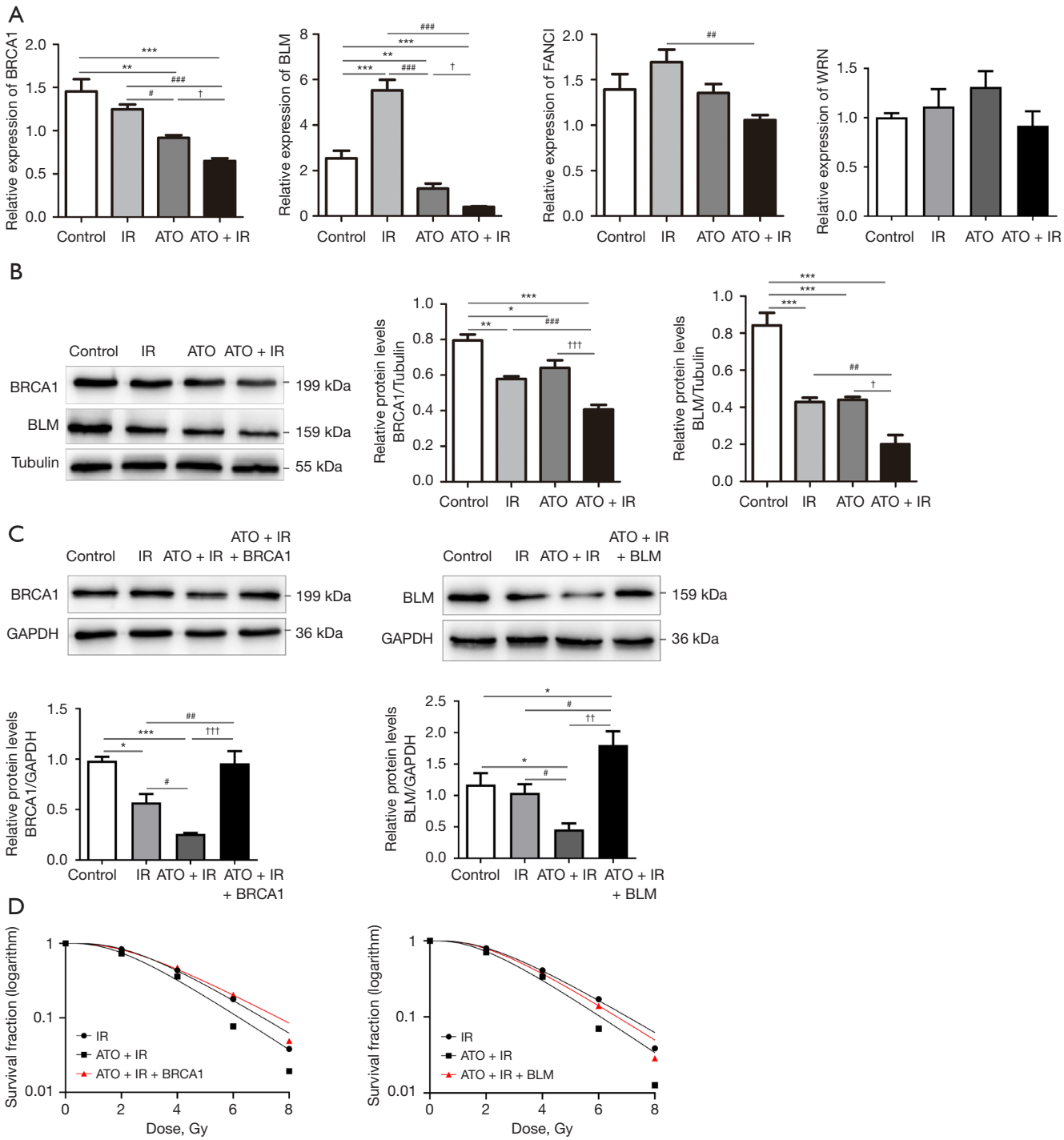

Figure 6 The radiosensitizing effect of ATO was facilitated by its interference with the DNA repair mechanism. (A) qRT-PCR validation of the relative expression of BRCA1, BLM, FANCI, and WRN in the indicated treatment. (B,C) Representative Western blots of BRCA1 and BLM in the indicated treatment (left panel) and Western blotting analysis of BRCA1 and BLM (right panel). GAPDH was used as the loading control (n=3). *, P<0.05; **, P<0.01; ***, P<0.001 *vs.* control group; $^{\#}$, P<0.05; $^{\#\#}$, P<0.01; $^{\#\#\#}$, P<0.001 *vs.* IR group; †, P<0.05; ††, P<0.01; †††, P<0.001 *vs.* ATO group. (D) Radiosensitization effect of the indicated treatment evaluated via clonogenic assay. Data are representative of three independent experiments (n=3). ATO, arsenic trioxide; BLM, bloom syndrome protein; BRCA1, breast cancer 1; GAPDH, glyceraldehyde 3-phosphate dehydrogenase; IR, irradiation; qRT-PCR, quantitative real-time polymerase chain reaction.

Table 4 Main parameters of SiHa cell survival curve after the overexpression of BRCA1

Group	D0 (Gy)	Dq (Gy)	SER
IR	1.90	2.77	–
ATO + IR	1.77	2.10	1.32
ATO + IR + BRCA1	2.05	3.11	0.90

D0: mean lethal dose. Dq: quasithreshold dose. ATO, arsenic trioxide; BRCA1, breast cancer 1; IR, irradiation; SER, sensitizer enhancement ratio.

Table 5 Principal parameters of SiHa cell survival curve after the overexpression of BLM1

Group	D0 (Gy)	Dq (Gy)	SER
IR	1.98	2.55	–
ATO + IR	1.75	2.01	1.27
ATO + IR + BLM	1.86	2.44	1.04

D0: mean lethal dose. Dq: quasithreshold dose. ATO, arsenic trioxide; BLM, bloom syndrome protein; IR, irradiation; SER, sensitizer enhancement ratio.

related adverse events reducing patients' quality of life and treatment continuity. Therefore, developing more effective treatment strategies is a critical direction in clinical research. In this study, we investigated the anticancer effect of ATO on CC cells, confirming its radiosensitizing activity and further discovering that its underlying mechanism involves inhibition of DNA damage repair pathway. Our findings present a novel method for the treatment of CC and provide theoretical and experimental evidence for the application of ATO in CC therapy.

ATO has been used in the treatment of APL for many years and is recognized as a safe and well-established antitumor agent. Its side effects are relatively well-defined, primarily including prolongation of the QTc interval, leukocytosis, and hepatotoxicity, but they are generally controllable and rarely result in severe adverse events. These effects can typically be mitigated by reducing the concentration of the drug administered. Numerous studies have indicated that a dosage of 2 μM or 0.2 mg/kg is considered a safe threshold for ATO administration (23-25). Below this concentration, ATO does not significantly inhibit cell growth but can contribute to tumor suppression when used in combination with other therapeutic modalities (26). These findings suggest that when combining ATO with radiotherapy, its dosage can be appropriately reduced, thereby ensuring the therapeutic efficacy against tumors while minimizing the side effects of the drug. Our results confirmed that a concentration of 1 μM of ATO could significantly enhance the sensitivity of CC cells to radiotherapy while causing only a minimal amount of cell death (*Figure 1*).

Human papillomavirus (HPV) infection, especially with high-risk types like HPV16 and HPV18, drives carcinogenesis by integrating viral oncogenes (E6/E7) into the host genome. Both SiHa and HeLa cell lines come from CC but have different HPV infection statuses. SiHa cells have the HPV16 genome integrated (1–2 copies), with constant E6/E7 oncogene expression. In contrast, HeLa cells have about 50 copies of the HPV18 genome integrated, featuring high E6/E7 expression and genomic instability (27). In SiHa and HeLa cells, HPV infection promotes malignancy through shared mechanisms like genomic instability, loss of proliferation control, apoptosis resistance, and immune evasion [(I) Human malignancies associated with persistent HPV infection. (II) Molecular mechanisms underlying human papillomavirus E6 and E7 oncoprotein-induced cell transformation. (III) Role of IL-10 and TGF-β1 in local immunosuppression in HPV-associated cervical neoplasia.]. However, it differs in integration complexity, pathway activation, and therapeutic responses. HeLa cells, driven by HPV18, are more adaptable to stress (e.g., radiation), making them suitable for studying metastasis and chemotherapy resistance. SiHa cells, infected with HPV16, better reflect early carcinogenic events and are ideal for studying them. In our study, we also found that ATO's radiosensitizing effect was more significant in SiHa cells than HeLa cells, so the following xenograft model uses SiHa cells.

We further evaluated the toxic effect of ATO in mice. During the course of treatment, no discernible side effects, including diarrhea, weight loss, or unexpected mortality, were observed. Additionally, no significant pathological changes were detected in various organs (data not shown), indicating that ATO could also exert a pronounced radiosensitizing effect at nontoxic doses.

Furthermore, compared with platinum-based drugs, ATO has a significant advantage in that it does not lead to pronounced bone marrow suppression (28-30). Bone marrow suppression is one of the most common toxic side effects of chemoradiotherapy, causing severe damage to the hematopoietic system, disrupting the bone marrow microenvironment, and leading to a variety of issues such as infections, bleeding, anemia, and even multiple organ

failure. Severe bone marrow suppression can lead to the suspension or termination of patient treatment, thereby reducing or even causing treatment failure (31-33). Bone marrow suppression is also a key contributor for the poor efficacy of CCRT based on platinum drugs for CC. Therefore, researchers have been striving to develop methods to alleviate bone marrow suppression during chemoradiotherapy for some time. As ATO does not cause bone marrow suppression, it is an attractive therapeutic choice. We thus hypothesized that compared with the commonly used platinum-based drugs, ATO can greatly reduce the severity of bone marrow suppression during CCRT, improve patient tolerance to CCRT, and thus ensure the maximum therapeutic effect.

Radiotherapy is one of the primary treatments for cancer (34), the core mechanism of which is the use of high-energy radiation to damage the DNA of cancer cells, resulting in DSBs (35). If this damage is not promptly repaired or repaired in a manner that inhibits subsequent replication, cell cycle arrest, apoptosis, or necrosis may be triggered. However, cancer cells uniformly possess efficient DNA damage repair mechanisms that can quickly respond to and repair these injuries, thereby escaping the cytotoxic effects of radiotherapy. Homologous recombination (HR) and nonhomologous end joining (NHEJ) represent the two primary DNA damage repair pathways that respond to IR (36). HR is a more accurate method for repairing DNA DSBs, requiring a homologous template (usually a sister chromatid). It occurs during the S and G2 phases of the cell cycle and involves genes of the Rad52 epistasis group and *BRCA1/2*, exonuclease 1 (*EXO1*), *BLM*, *WRN*, and checkpoint kinase 1 (*CHEK1*), among others (37-39). In contrast, NHEJ does not require a homologous template and instead directly ligates the broken DNA ends. Although this process may introduce small insertions or deletions, it efficiently restores the continuity of the DNA strand. It is particularly active during the G0 and G1 phases of the cell cycle and involves the core components DNA-PKcs/Ku70/Ku80 and DNA ligase IV/XRCC4/XLF (40,41).

ATO has been demonstrated to be able to induce DSBs and cause chromosomal aberrations (42,43). Our data also indicated that ATO treatment induces significant DNA damage. Moreover, when combined with IR, ATO could induce much more severe DNA damage as compared to IR only, which explains why ATO enhances the cytotoxic effect of IR and somewhat clarifies the underlying mechanism of the radiosensitizing effect of ATO. Previous studies have confirmed that ATO impedes the repair of DNA DSBs and affects the selection of pathways involved in DNA DSB repair. Various studies have demonstrated that cells exposed to ATO preferentially are repaired using the "error prone" NHEJ, with repair by the error-free HR pathways being inhibited (44-46). In this study, we found that ATO significantly decreased the protein level of BRCA1 and BLM, two key proteins in HR, also suggesting an impairment of the HR pathway that has been reported in previous work (44-46). Less DNA damage repair results in greater cell death. Although DSBs can be repaired via the NHEJ pathway, the inherent error-prone nature of this mechanism can result in a higher incidence of misrepair events. This consequently augments the propensity for genomic instability, thereby increasing the probability of cellular demise.

By mediating HR, BRCA1 plays a crucial role in DNA DSB repair, thereby ensuring genomic stability, which is also pivotal in tumor suppression (47,48). There is also research indicating that germline variants of HR genes, including BRCA1, are associated with CC (49). However, the precise role of BRCA1 in CC remains to be fully delineated, with the interplay between BRCA1 and the prognostic outcomes of CC still being a matter of considerable controversy. Some studies have indicated that BRCA1 deficiency is associated with an adverse prognosis in CC (50,51). Interestingly, conflicting results have been reported in other studies; for instance, Balacescu *et al.* found that the overexpression of BRCA1 and BRCA2 in patients with advanced CC was correlated with treatment failure (52). Furthermore, recent *in vitro* research by Wen *et al.* suggested that that the overexpression of BRCA1 could contribute to the heightened chemoradiation resistance observed in cervical squamous cell carcinoma (53). In our study, a reduction in BRCA1 protein levels was observed in conjunction with an augmented tumoricidal effect subsequent to combined treatment with ATO and IR, indicating a potential association between diminished BRCA1 expression and improved therapeutic efficacy. This observation implies that CC cells with lower BRCA1 expression may exhibit increased sensitivity to the combined treatment modality of ATO and IR, thus potentially serving as a predictive biomarker for treatment efficacy in this context.

Conclusions

In summary, our study demonstrates that ATO significantly enhances the radiosensitivity of CC both *in vitro* and *in vivo*.

Mechanistically, ATO augmented radiation-induced G2/M phase arrest and apoptosis, thereby amplifying the cancer-killing effects of ionizing radiation. Furthermore, ATO disrupted DNA damage repair pathways by suppressing key repair genes, including BRCA1 and BLM, as evidenced by reduced γH2AX foci and downregulation of DNA repair-related transcripts and proteins. Critically, overexpression of BRCA1 or BLM reversed the radiosensitizing effect of ATO, confirming its reliance on impairing DNA repair mechanisms. Our findings highlight ATO as a promising radiosensitizer for CC therapy, particularly through its dual role in exacerbating DNA damage and inhibiting repair processes. Future studies should explore the translational potential of ATO in clinical radiotherapy regimens and validate its efficacy across broader cancer models.

Acknowledgments

None.

Footnote

Reporting Checklist: The authors have completed the ARRIVE and MDAR reporting checklists. Available at https://tcr.amegroups.com/article/view/10.21037/tcr-2025-450/rc

Data Sharing Statement: Available at https://tcr.amegroups.com/article/view/10.21037/tcr-2025-450/dss

Peer Review File: Available at https://tcr.amegroups.com/article/view/10.21037/tcr-2025-450/prf

Funding: This study was supported by the Maternal and Child Health Research Project of Jiangsu Province (No. F202035), and the Medical Science and Technology Innovation Project of Xuzhou Municipal Health Commission (No. XWKYHT20220074). The funding agencies were not involved in the study design, collection, analysis and interpretation of data, or in the drafting of the manuscript.

Conflicts of Interest: All authors have completed the ICMJE uniform disclosure form (available at https://tcr.amegroups.com/article/view/10.21037/tcr-2025-450/coif). The authors have no conflicts of interest to declare.

Ethical Statement: The authors are accountable for all aspects of the work in ensuring that questions related to the accuracy or integrity of any part of the work are appropriately investigated and resolved. Experiments were performed under a project license (No. 202305T019) granted by the approval of the Animal Care and Use Committee of Xuzhou Medical University, in compliance with national guidelines for the care and use of animals.

References

1. Arbyn M, Weiderpass E, Bruni L, et al. Estimates of incidence and mortality of cervical cancer in 2018: a worldwide analysis. Lancet Glob Health 2020;8:e191-203.
2. Bhatla N, Aoki D, Sharma DN, et al. Cancer of the cervix uteri. Int J Gynaecol Obstet 2018;143 Suppl 2:22-36.
3. Hu K, Wang W, Liu X, et al. Comparison of treatment outcomes between squamous cell carcinoma and adenocarcinoma of cervix after definitive radiotherapy or concurrent chemoradiotherapy. Radiat Oncol 2018;13:249.
4. Li J, Li Y, Wang H, et al. Neoadjuvant chemotherapy with weekly cisplatin and paclitaxel followed by chemoradiation for locally advanced cervical cancer. BMC Cancer 2023;23:51.
5. Zhang C, Xu C, Gao X, et al. Platinum-based drugs for cancer therapy and anti-tumor strategies. Theranostics 2022;12:2115-32.
6. Waxman S, Anderson KC. History of the development of arsenic derivatives in cancer therapy. Oncologist 2001;6 Suppl 2:3-10.
7. Zhang TD, Chen GQ, Wang ZG, et al. Arsenic trioxide, a therapeutic agent for APL. Oncogene 2001;20:7146-53.
8. Sun HD, Ma L, Hu XC, et al. Ai-lin 1 treated 32 cases of acute promyelocytic leukemia. Chin J Integrat Chin West Med 1992;12:170-1.
9. Munshi NC, Tricot G, Desikan R, et al. Clinical activity of arsenic trioxide for the treatment of multiple myeloma. Leukemia 2002;16:1835-7.
10. Hoonjan M, Jadhav V, Bhatt P. Arsenic trioxide: insights

into its evolution to an anticancer agent. J Biol Inorg Chem 2018;23:313-29.
11. Diepart C, Karroum O, Magat J, et al. Arsenic trioxide treatment decreases the oxygen consumption rate of tumor cells and radiosensitizes solid tumors. Cancer Res 2012;72:482-90.
12. Jutooru I, Chadalapaka G, Sreevalsan S, et al. Arsenic trioxide downregulates specificity protein (Sp) transcription factors and inhibits bladder cancer cell and tumor growth. Exp Cell Res 2010;316:2174-88.
13. Stevens JJ, Graham B, Dugo E, et al. Arsenic Trioxide Induces Apoptosis via Specific Signaling Pathways in HT-29 Colon Cancer Cells. J Cancer Sci Ther 2017;9:298-306.
14. Kroemer G, de Thé H. Arsenic trioxide, a novel mitochondriotoxic anticancer agent? J Natl Cancer Inst 1999;91:743-5.
15. Li YM, Broome JD. Arsenic targets tubulins to induce apoptosis in myeloid leukemia cells. Cancer Res 1999;59:776-80.
16. Sun Z, Li M, Bai L, et al. Arsenic trioxide inhibits angiogenesis in vitro and in vivo by upregulating FoxO3a. Toxicol Lett 2019;315:1-8.
17. Sun Z, Cao Y, Xing Y, et al. Antiangiogenic effect of arsenic trioxide in HUVECs by FoxO3a-regulated autophagy. J Biochem Mol Toxicol 2021;35:e22728.
18. Lai YL, Chang HH, Huang MJ, et al. Combined effect of topical arsenic trioxide and radiation therapy on skin-infiltrating lesions of breast cancer-a pilot study. Anticancer Drugs 2003;14:825-8.
19. Kumar P, Gao Q, Ning Y, et al. Arsenic trioxide enhances the therapeutic efficacy of radiation treatment of oral squamous carcinoma while protecting bone. Mol Cancer Ther 2008;7:2060-9.
20. Tang R, Zhu J, Liu Y, et al. Formulation Comprising Arsenic Trioxide and Dimercaprol Enhances Radiosensitivity of Pancreatic Cancer Xenografts. Technol Cancer Res Treat 2021;20:15330338211036324.
21. Ninomiya Y, Yu D, Sekine-Suzuki E, et al. Synergistic Effects of Arsenite on Radiosensitization of Glioblastoma Cells. Anticancer Res 2017;37:4111-7.
22. Cai Y, Zhu C, Lu S, et al. Arsenic sulfide enhances radiosensitivity in rhabdomyosarcoma via activating NFATc3-RAG1 mediated DNA double strand break (DSB). Chem Biol Interact 2024;399:111149.
23. Ardalan B, Subbarayan PR, Ramos Y, et al. A phase I study of 5-fluorouracil/leucovorin and arsenic trioxide for patients with refractory/relapsed colorectal carcinoma. Clin Cancer Res 2010;16:3019-27.
24. Cohen KJ, Gibbs IC, Fisher PG, et al. A phase I trial of arsenic trioxide chemoradiotherapy for infiltrating astrocytomas of childhood. Neuro Oncol 2013;15:783-7.
25. Fang Y, Zhang Z. Arsenic trioxide as a novel anti-glioma drug: a review. Cell Mol Biol Lett 2020;25:44.
26. Fang Y, Bai Z, Cao J, et al. Low-intensity ultrasound combined with arsenic trioxide induced apoptosis of glioma via EGFR/AKT/mTOR. Life Sci 2023;332:122103.
27. Wang Z, Liu C, Liu W, et al. Long-read sequencing reveals the structural complexity of genomic integration of HPV DNA in cervical cancer cell lines. BMC Genomics 2024;25:198.
28. Adès L, Thomas X, Bresler AG, et al. Arsenic trioxide is required in the treatment of newly diagnosed acute promyelocytic leukemia. Analysis of a randomized trial (APL 2006) by the French Belgian Swiss APL group. Haematologica 2018;103:2033-9.
29. Cicconi L, Lo-Coco F. Current management of newly diagnosed acute promyelocytic leukemia. Ann Oncol 2016;27:1474-81.
30. Glass JL, Derkach A, Hilden P, et al. Arsenic trioxide therapy predisposes to herpes zoster reactivation despite minimally myelosuppressive therapy. Leuk Res 2021;106:106569.
31. Epstein RS, Aapro MS, Basu Roy UK, et al. Patient Burden and Real-World Management of Chemotherapy-Induced Myelosuppression: Results from an Online Survey of Patients with Solid Tumors. Adv Ther 2020;37:3606-18.
32. Epstein RS, Weerasinghe RK, Parrish AS, et al. Real-world burden of chemotherapy-induced myelosuppression in patients with small cell lung cancer: a retrospective analysis of electronic medical data from community cancer care providers. J Med Econ 2022;25:108-18.
33. Zhou C, Wang Z, Sun Y, et al. Sugemalimab versus placebo, in combination with platinum-based chemotherapy, as first-line treatment of metastatic non-small-cell lung cancer (GEMSTONE-302): interim and final analyses of a double-blind, randomised, phase 3 clinical trial. Lancet Oncol 2022;23:220-33.
34. Barton MB, Jacob S, Shafiq J, et al. Estimating the demand for radiotherapy from the evidence: a review of changes from 2003 to 2012. Radiother Oncol 2014;112:140-4.
35. Lemaître C, Soutoglou E. DSB (Im)mobility and DNA repair compartmentalization in mammalian cells. J Mol Biol 2015;427:652-8.
36. Chang HHY, Pannunzio NR, Adachi N, et al. Non-homologous DNA end joining and alternative pathways to double-strand break repair. Nat Rev Mol Cell Biol

2017;18:495-506.
37. Thompson LH, Schild D. Recombinational DNA repair and human disease. Mutat Res 2002;509:49-78.
38. Thorslund T, West SC. BRCA2: a universal recombinase regulator. Oncogene 2007;26:7720-30.
39. Salunkhe S, Daley JM, Kaur H, et al. Promotion of DNA end resection by BRCA1-BARD1 in homologous recombination. Nature 2024;634:482-91.
40. Nussenzweig A, Nussenzweig MC. A backup DNA repair pathway moves to the forefront. Cell 2007;131:223-5.
41. van Gent DC, van der Burg M. Non-homologous end-joining, a sticky affair. Oncogene 2007;26:7731-40.
42. Dong JT, Luo XM. Arsenic-induced DNA-strand breaks associated with DNA-protein crosslinks in human fetal lung fibroblasts. Mutat Res 1993;302:97-102.
43. Jiménez-Villarreal J, Rivas-Armendariz DI, Pineda-Belmontes CP, et al. Detection of damage on single- or double-stranded DNA in a population exposed to arsenic in drinking water. Genet Mol Res 2017;16. doi: 10.4238/gmr16029241.
44. Kurosawa A, Saito S, Sakurai M, et al. Arsenic affects homologous recombination and single-strand annealing but not end-joining pathways during DNA double-strand break repair. FEBS J 2023;290:5313-21.
45. Morales ME, Derbes RS, Ade CM, et al. Heavy Metal Exposure Influences Double Strand Break DNA Repair Outcomes. PLoS One 2016;11:e0151367.
46. Matthäus T, Stößer S, Seren HY, et al. Arsenite Impairs BRCA1-Dependent DNA Double-Strand Break Repair, a Mechanism Potentially Contributing to Genomic Instability. Int J Mol Sci 2023;24:14395.
47. Zhang J, Powell SN. The role of the BRCA1 tumor suppressor in DNA double-strand break repair. Mol Cancer Res 2005;3:531-9.
48. Venkitaraman AR. Cancer suppression by the chromosome custodians, BRCA1 and BRCA2. Science 2014;343:1470-5.
49. Kokemüller L, Ramachandran D, Schürmann P, et al. Germline variants of homology-directed repair or mismatch repair genes in cervical cancer. Int J Cancer 2025;156:700-10.
50. Paik ES, Chang CS, Chae YL, et al. Prognostic Relevance of BRCA1 Expression in Survival of Patients With Cervical Cancer. Front Oncol 2021;11:770103.
51. Narayan G, Arias-Pulido H, Koul S, et al. Frequent promoter methylation of CDH1, DAPK, RARB, and HIC1 genes in carcinoma of cervix uteri: its relationship to clinical outcome. Mol Cancer 2003;2:24.
52. Balacescu O, Balacescu L, Tudoran O, et al. Gene expression profiling reveals activation of the FA/BRCA pathway in advanced squamous cervical cancer with intrinsic resistance and therapy failure. BMC Cancer 2014;14:246.
53. Wen X, Liu S, Cui M. Effect of BRCA1 on the Concurrent Chemoradiotherapy Resistance of Cervical Squamous Cell Carcinoma Based on Transcriptome Sequencing Analysis. Biomed Res Int 2020;2020:3598417.

(English Language Editor: J. Gray)

Cite this article as: Gao X, Liu G, Zhao Z, Tang Y, Hui H, Wang C, Li D, Ma Y, Sun Z, Zhou Y. Arsenic enhances cervical cancer cell radiosensitivity by suppressing the DNA damage repair pathway. Transl Cancer Res 2025;14(3):2078-2094. doi: 10.21037/tcr-2025-450